Published in final edited form as:
J Comp Neurol. 2012 October 1; 520(14): 3256–3276. doi:10.1002/cne.23096.

Role of Retinal Input on the Development of Striate–Extrastriate Patterns of Connections in the Rat

R.J. Laing[1], **A.S. Bock**[1], **J. Lasiene**[2], and **J.F. Olavarria**[1,*]

[1]Department of Psychology, and Behavior and Neuroscience program, University of Washington, Seattle, Washington 98195–1525

[2]Laboratory for Motor Neuron Disease, RIKEN Brain Science Institute, Saitama 351–0198, Japan

Abstract

Previous studies have shown that retinal input plays an important role in the development of interhemispheric callosal connections, but little is known about the role retinal input plays on the development of ipsilateral striate–extrastriate connections and the interplay that might exist between developing ipsilateral and callosal pathways. We analyzed the effects of bilateral enucleation performed at different ages on both the distribution of extrastriate projections originating from restricted loci in medial, acallosal striate cortex, and the overall pattern of callosal connections revealed following multiple tracer injections. As in normal rats, striate–extrastriate projections in rats enucleated at birth consisted of multiple, well-defined fields that were largely confined to acallosal regions throughout extrastriate cortex. However, these projections were highly irregular and variable, and they tended to occupy correspondingly anomalous and variable acallosal regions. Moreover, area 17, but not area 18a, was smaller in enucleates compared to controls, resulting in an increase in the divergence of striate projections. Anomalies in patterns of striate–extrastriate projections were not observed in rats enucleated at postnatal day (P)6, although the size of area 17 was still reduced in these rats. These results indicate that the critical period during which the eyes influence the development of striate–extrastriate, but not the size of striate cortex, ends by P6. Finally, enucleation did not change the time course and definition of the initial invasion of axons into gray matter, suggesting that highly variable striate projections patterns do not result from anomalous pruning of exuberant distributions of 17–18a fibers in gray matter.

Indexing Terms

corticocortical projections; intrahemispheric; interhemispheric; visual cortex; feedforward; feedback; critical period; sensitive period; plasticity; enucleation; deprivation; deafferentation

---

During embryonic development, occipital cortex becomes parcellated into striate cortex (area 17, primary visual cortex, V1), and a number of extrastriate areas that will later acquire more or less complete representations of the opposite visual hemifield. During a subsequent phase of development, topographically organized intrahemispheric connections are established between striate cortex and extrastriate areas, as well as between sets of extrastriate areas, giving rise to hierarchical networks specialized in the processing of specific attributes of the visual scene (Van Essen and Maunsell, 1983; Maunsell, 1992; Wang et al., 2011). In addition, highly specific patterns of interhemispheric callosal

[*]Correspondence to: J.F. Olavarria, Department of Psychology, University of Washington, Box 351525, Seattle, WA 98195-1525. jaime@uw.edu.

connections develop between visual areas in both hemispheres (Olavarria and Van Sluyters, 1985; Innocenti, 1991). What determines the topographic organization of intra- and interhemispheric connections? Studies in anophthalmic rodents (Olavarria et al., 1984, 1988; Bravo and Inzunza, 1994) have shown that the distributions of both striate–extrastriate and visual callosal connections are abnormal in these animals, indicating that the eyes play an important role in the specification of these pathways. Early retinal deafferentation also affects the development of corticocortical connections in other species, including monkeys (Dehay et al., 1989, 1996), cats (Innocenti and Frost, 1980; Olavarria and Van Sluyters, 1995), hamsters (Rhoades and Dellacroce, 1980; Fish et al., 1991; O'Brien and Olavarria, 1995), and opossum (Karlen et al., 2006).

However, studies of visual callosal patterns in rats and mice have revealed that the eyes are necessary only during a brief time at the beginning of pathway formation, rather than during the entire developmental period (Olavarria et al., 1987; Olavarria and Hiroi, 2003). These authors showed that although the callosal pathway is very immature at postnatal day 6 (P6) (Olavarria and Van Sluyters, 1985), removal of the eyes at this age or later does not prevent the development of normal callosal patterns. In contrast, removal of the eyes at P4 or earlier results in patterns that are strikingly abnormal in both their overall distributions and point-to-point topography (Olavarria et al., 1987; Olavarria and Hiroi, 2003). These and similar studies in the ferret (Bock et al., 2012) show that lack of retinal input during a brief period induces permanent alterations in the overall distribution and topography of the visual callosal pathway. Thus, the period identified by delaying enucleation represents a unique developmental stage during which retinal input is critically needed for specifying the normal layout and topography of corticocortical connections. Mapping out this critical period is therefore important for identifying the retinally driven mechanisms that operate at this developmental stage, and for investigating how they lay down the blueprints for normal maps of corticocortical connectivity.

The term *critical period* used here refers to a well-defined developmental stage during which presence of a specific factor (in this case the retinae) is critically required (hence *critical* period) for development to proceed normally (Erzurumlu and Killackey, 1982). These critical periods typically occur at early stages of development, and have been described in various systems at different levels of the neuroaxis (see, e.g., Belford and Killackey, 1980). It is important to note that these critical periods differ from periods occurring later in life, during which functional and anatomical changes reflect changes in sensory experience that do not necessarily require end organ damage (Erzurumlu and Killackey, 1982). For example, in rat visual cortex vision deprivation experiments have demonstrated a period of ocular dominance plasticity that extends approximately from P18 to well into the second month of life (Fagiolini et al., 1994). Unfortunately, as pointed out by Erzurumlu and Killackey (1982), the terms *critical period* and *sensitive period* have been used interchangeably to refer to periods that appear to correspond to temporally and mechanistically distinct phases of development (see, e.g., Crowley and Katz, 2000).

Most studies of the effects of retinal deafferentation on the development of visual corticocortical connections have focused on the visual callosal pathway (Olavarria et al., 1987; Olavarria and Li, 1995; Olavarria and Hiroi, 2003). Thus, little information is available about the susceptibility of striate–extrastriate connections to neonatal enucleation, and whether or not the effects of enucleation on these connections resemble in some manner those of the callosal pattern. In the present study we therefore examined the effects that early enucleation has on the overall organization of striate–extrastriate connections. We addressed the following questions in a group of adult rats bilaterally enucleated at birth: Are projections emerging from restricted loci in striate cortex of enucleated rats patchy as in control rats, or are they distributed in a diffuse fashion? If patchy, do the patches form

consistent projection patterns associated with known subdivisions of extrastriate cortex? Are the abnormalities observed in the feedforward projection also present in the feedback extrastriate–striate pathway? Do striate–extrastriate projections originating from acallosal striate cortex maintain a close, complementary relationship with callosal connections in enucleated animals, as they do in normal rats? Finding that anomalies in striate–extrastriate connections correlate closely with anomalies in the callosal pathway would suggest that the eyes guide the development of both inter- and intrahemispheric connections through common, or linked, mechanisms.

In a second group of animals we delayed the age at which enucleation was performed in order to determine whether the critical period for the effect of enucleation on the pattern of striate–extrastriate projections is similar to that for callosal connections. A recent study in mice showed that feedback pathways develop later than striate–extrastriate feedforward projections (Dong et al., 2004), raising the possibility that the critical period for feedback extrastriate–striate projections is delayed with respect to that for the feedforward, striate–extrastriate projections. To test this possibility, in some animals we injected striate cortex with both anterogradely and retrogradely transported tracers to investigate the effect of delayed enucleation on the distribution and critical period of both feedforward and feedback pathways. We also assessed the effect of delayed enucleation on the size of visual cortex (Olavarria et al., 1987) in order to compare the critical periods for the effects of enucleation on the pattern of striate–extrastriate projections and on the size of visual cortex. Finally, in a third experimental group we examined the initial growth of striate–extrastriate projections into gray matter of young pups enucleated at birth to assess whether the definition and time course of the initial invasion of axons into gray matter differs from a recent description of the development of these projections in normal rats (Ruthazer et al., 2010).

Materials and Methods

Our study is based on data obtained from a total of 36 Long–Evans pigmented rats. Pregnant animals were monitored several times daily and the births of the litters were determined to within 12 hours. Twenty-eight rat pups were anesthetized with isoflurane (2–4% in air) and binocularly enucleated either within 24 hours of birth (BE0, $n = 17$) or at the following postnatal ages: P4 (BE4, $n = 6$) and P6 (BE6, $n = 5$). After recovering from the anesthesia, pups were returned to their dams. Enucleations at P4 and P6 were performed to determine when enucleation no longer affects the development of striate–extrastriate projections. These ages were chosen because previous studies in the rat have shown that the period during which development of callosal connections depends on retinal input ends by P6 (Olavarria and Hiroi, 2003). In addition, eight rats were used for analyzing striate–extrastriate projections in normal adult animals. All surgical procedures were performed according to protocols approved by the Institutional Animal Care and Use Committee (IACUC) at the University of Washington.

Tracer injections

In both control and enucleated animals, patterns of striate–extrastriate projections were analyzed in tangential sections through the flattened cortical hemisphere following restricted tracer injections into striate cortex, while the distribution of callosal connections was revealed in the same hemisphere following multiple injections of a different tracer in the opposite hemisphere. In some animals, brains were analyzed in the coronal plane. In normal rats, callosal connections occupy approximately the lateral third of area 17, while in area 18a they form more or less continuous bands on either side of this area, as well as a series of callosal bridges dividing area 18a in a number of compartments that correspond closely to visual areas described physiologically (Montero, 1973; Montero et al., 1973a,b; Espinoza

and Thomas, 1983; Olavarria and Montero, 1984; Olavarria and Van Sluyters, 1985; Thomas and Espinoza, 1987). Callosal and callosal-free regions have also been described in striate and extrastriate cortex of enucleated rats (Olavarria et al., 1987). To facilitate the description of procedures and results, in the present report we use the terms “callosal” or “acallosal” to refer to regions in striate and extrastriate cortex that either contain, or are largely devoid of callosal connections, respectively. For reasons explained in the Discussion, here we describe patterns of striate–extrastriate projections resulting from tracer injections aimed at acallosal regions of striate cortex. Anatomical experiments in all normally reared animals (n = 8) and in 22 rats enucleated at different postnatal ages took place when they were at least 1 month old. In addition, six rats enucleated at P0 were injected either at P4 (n = 3) or P6 (n = 3) and studied at P6 or P8, respectively. Tracer injections were made under isoflurane anesthesia (2–4% in air). To study the patterns of striate-extrastriate projections, all animals received a single injection of biotinylated dextran amine (BDA, 10% in DW, Molecular Probes, Eugene, OR), which is predominantly transported anterogradely. To reveal the pattern of feedback extrastriate-striate projections, some control and enucleated animals studied at adulthood also received restricted injection of fluorescent tracers (rhodamine beads, RB, or green beads, GB; LumaFluor, Naples, FL, concentrated stock solution), which are transported retrogradely. Small volumes (0.05–0.1 μl) of BDA or fluorescent tracers were injected into striate cortex of the right hemisphere (adults: ≈2.9–3.5 mm from the midline; 0.1–1.7 mm anterior to the lambda suture; neonates: ≈3.0 mm from the midline and 0.5 mm anterior to the lambda suture). In all cases analyzed the tracer injections were restricted to gray matter. To reveal the overall pattern of callosal connections, multiple (12–15) injections (total volume ≈4.0 μL) of horseradish peroxidase (HRP, Sigma, St. Louis, MO; 25% in saline) were placed over visual cortex of the left hemisphere (Olavarria and Van Sluyters, 1985). All tracers were pressure-injected through glass micropipettes (50–100 μm tip diameter).

Histochemical processing

After a survival period of 2 days the animals were deeply anesthetized with pentobarbital sodium (100 mg/kg intraperitoneally) and perfused through the heart with 0.9% saline followed by 4% paraformaldehyde in 0.1 M phosphate buffer (PB, pH 7.4). After being removed from the skull, the brains from adult control and enucleated rats were analyzed in histological sections cut either tangentially to the flattened cortex (control, n = 5, enucleated, n = 19) or in the coronal plane (control, n = 3, enucleated, n = 3). All brains of rats perfused at P6 (n = 3) or P8 (n = 3) were studied in coronal sections. In the cases studied in the tangential plane, the cortical mantle of the injected hemisphere was separated from the brainstem, flattened between glass slides, and left overnight in 0.1M PB, while the thalamus was left overnight in 20% sucrose in 0.1M PB. The flattening procedure was done with great care to ensure that both striate and extrastriate cortices were contained in the tangential sections. The following day flattened cortices were removed from the glass slides and placed in 30% sucrose in 0.1M PB for 1 hour and 60-μm thick sections were cut tangential to the cortical surface using a freezing microtome. The thalamus was cut into 60-μm thick coronal sections. Brains to be studied in the coronal plane were left overnight in 20% sucrose and 0.1 M PB. In adult brains the data were analyzed in a series of 60-μ thick coronal sections, while in neonate rats the sections were 80-μm thick. If present in the same brain, fluorescent and BDA labeling patterns were analyzed in alternate series of sections. Sections in the series examined only for fluorescence were mounted on slides and analyzed under epifluorescence without further processing. However, sections in the series processed for BDA were often also analyzed for epifluorescence because the fluorescent labeling in these sections was similar to that in sections not processed for BDA. This allowed a direct correlation of the spatial location of retrograde and anterograde labeling in the same section. The sites injected with fluorescent tracers often appeared as dark areas in the sections

processed for BDA (sites marked with asterisks in Fig. 1). However, inspection of BDA labeling patterns in target areas revealed that BDA had not been uptaken at these sites, indicating that the dark staining at these sites was artifactual. For instance, Figure 7B,C shows that fields of fluorescently labeled cells were displaced with respect of BDA-labeled fields in accordance with the topography of extrastriate visual areas (see Results). In contrast, when both tracers were injected at adjacent sites, the fields labeled by each tracer tended to overlap with each other (Fig. 7A). Similarly, if uptake of BDA had occurred at the fluorescent injection sites, two or more BDA-labeled fields, instead of one, would be observed in the dorsal lateral geniculate nucleus (dLGN), but this was not the case (Fig. 1). A detailed account of the data from multiple tracer injections in striate cortex will be part of a future report. BDA labeling was revealed using the standard Avidin-Biotin-Peroxidase protocol (Vectastain Elite ABC kit, Vector Laboratories, Burlingame, CA) and 0.01% H_2O_2 in 0.05% 3-3′ diaminobenzidine, with cobalt or nickel intensification; sections were then mounted, dehydrated, defatted, and coverslipped. In the young rats studied, we assumed that the pattern of projections revealed with BDA is that present at the time of perfusion (Simon and O'Leary, 1992). HRP labeling was revealed using tetramethyl benzidine as the chromogen (Mesulam, 1978).

Data acquisition and analysis

Digital images of the BDA and HRP labeling patterns in tangential sections were obtained by scanning the sections at 2400 dpi using an Epson 4990 scanner. These data were used for characterizing the effect of enucleation on these patterns, and for measuring the size of the overall BDA-labeled projection in area 18a. High-magnification images of selected BDA-labeled fields in tangential or coronal sections were obtained using a Leica light microscope coupled to a digital camera. The distribution of cells labeled retrogradely with fluorescent tracers in adult rats, and of striate–extrastriate axons labeled anterogradely by BDA in neonatal rats were analyzed using a microscope equipped with a motorized stage (LEPCO) controlled by a Dell XPS T500 computer and a graphic system (Neurolucida, MicroBrightField, Williston, VT).

Identifying the borders of areas 17 and 18a—Previous studies have shown that scanning unstained sections can readily reveal myelin patterns (Richter and Warner, 1974; Bock and Olavarria, 2011), and we used this procedure to identify the borders of areas 17 and 18a (Krieg, 1946; Caviness, 1975; Zilles et al., 1980) in tangential sections from control and enucleated rats (Fig. 5; Olavarria and Van Sluyters, 1985; Olavarria et al., 1987). Immediately lateral to area 17 lays an area of less dense myelination (Fig. 5B; Olavarria and Van Sluyters, 1985), which previous studies have identified as area 18a (Krieg, 1946; Caviness, 1975). In normal rats, it is generally accepted that area 18a contains the visual areas that have been described in lateral extrastriate cortex of the rat, including the most lateral areas (areas laterointermediate, LI, and laterolateral, LL) (Montero, 1973, 1993; Montero et al., 1973a,b; Olavarria and Montero, 1981, 1984, 1989; Espinoza and Thomas, 1983; Thomas and Espinoza, 1987; Coogan and Burkhalter, 1993). Although myelination is less dense in visual cortex of enucleated animals (Olavarria et al., 1987), the lateral profile of area 18a can also be recognized in enucleated animals (Fig. 5F; Olavarria et al., 1987), and, as in normal rats, this area is the target of virtually all projections from striate cortex to lateral extrastriate cortex (see Results). Further information for identifying the location of the border of areas 17 and 18a in control and enucleated rats came from analyzing landmarks provided by the overall callosal pattern in visual cortex, and the relation that these landmarks have with the borders of areas 17 and 18a as revealed in the myelination patterns (Fig. 5; Olavarria and Van Sluyters, 1985; Olavarria et al., 1987). However, although the lateral border of area 18a can be readily recognized from myelin and callosal patterns, there are no clear criteria for recognizing the anterior border of this area. In order to

compare the size of area 18a across all experimental groups, we outlined an area that was identified using similar landmarks in normal and enucleated animals (see Fig. 4A). The lateral border of this area followed the lateral border of the myelinated region lying immediately lateral to area 17, as well as callosal bands overlapping this border and extending posteriorly, roughly parallel to the posterior half of the lateral border of area 17 (Fig. 5D,E). The anterior border of this area was drawn as a mediolateral line extending from the most anterior point in area 17 to the most posterior point of the barrel field, as visualized in the myelin or callosal pattern (Fig. 5), while its posterior border followed the edge of the histological section. Although similar in general shape and location, the area delimited by these criteria does not necessarily correspond exactly to areas "18a," "Oc2.1," or "Oc2L" of other studies (Krieg, 1946; Caviness, 1975; Zilles et al., 1980; Zilles and Wree, 1995).

Location and size of tracer injections in area 17—The location of the injection site determined with reference to the border of area 17 was confirmed by analyzing the distribution of retrogradely labeled fields within the ipsilateral dLGN (Montero et al., 1968; Godement et al., 1979; Kaiserman-Abramof et al., 1980; Guillery et al., 1985; Warton et al., 1988). We also estimated the size of the tracer injection in area 17 in order to analyze how the size of the tracer injection relative to the size of area 17 relates to the size of the overall projection in area 18a relative to the size of area 18a in both control and enucleated rats. In normal animals, estimates of the effective size of injections in visual cortex are usually obtained by measuring the sizes of the projections to targets such as the superior colliculus or dLGN. However, comparing injections sizes determined this way between control and enucleated animals would not be appropriate because thalamocortical connections are affected by neonatal enucleation in rodents (Warton et al., 1988). We therefore estimated the size of injections using two approaches based on the staining surrounding the injection sites. One approach consisted in outlining the perimeter where an abrupt transition in the staining density was observed. We also used the public domain NIH Image program (written by Wayne Rasband, National Institutes of Health [NIH], Bethesda, MD) to analyze density profiles at the injection sites obtained from digitized images of the BDA-processed tangential sections. We found that area measurements performed at 50% of the peak intensity level (after subtracting the background density value) were not significantly different ($P < 0.05$) from our estimates of the area encircled by the perimeter drawn around the injection site by visual inspection. The analysis performed using the NIH Image program was independent of adjustments in the contrast or other parameters of the digitized images. For each injection, the size used in our quantitative analysis was the average of the values obtained with these two approaches.

To illustrate the variability of striate–extrastriate projections in each experimental group, outlines of the injection sites and patterns of 17–18a projections in each group were superimposed and merged after they had been carefully aligned with reference to the location and orientation of the lateral border of area 17.

Quantitative analysis—Using Adobe Photoshop CS2 (Adobe Systems, San Jose, CA), digitized images of anatomical tracer and myelin labeling patterns from the same animal were carefully aligned with each other using the border of area 17, the edges of the sections, blood vessels, and other fiducial marks. To facilitate the quantitative analysis of the patterns of striate–extrastriate projections among the different experimental groups studied, thresholded version of these patterns were compared within and across groups. Thresholded versions of these patterns were prepared after first applying a median filter to reduce noise and a highpass filter to remove gradual changes in staining density across the entire image. The labeling density profiles were highly similar across cases, and no significant differences ($P < 0.05$) were found between groups in the mean, median, or range of pixel values. The

same filter parameters and thresholding levels were applied to all control and enucleated animals, and thresholded versions were visually inspected to confirm they accurately represented the labeling pattern observed in the tissue sections. Quantitative comparisons of the sizes of area 17, 18a, tracer injections, and projection patterns in area 18a were performed using an analysis of variance (ANOVA) with α set at 0.05; post-hoc comparisons were made using the Tukey HSD test. Figures were prepared using Adobe Photoshop CS2 and all imaging processing used, including contrast enhancement and intensity level adjustments, were applied to the entire images.

Results

Striate–extrastriate projections in normal rats and in rats enucleated at birth

Analysis of striate–extrastriate projections in normal and enucleated animals was performed in animals receiving single injections of an anterogradely transported tracer at restricted sites within acallosal regions of striate cortex. The pattern of striate–extrastriate projections in normal rats is illustrated in Figure 1A. As described previously (Olavarria and Montero, 1984; Coogan and Burkhalter, 1993; Montero, 1993), following single tracer injections, projections from striate cortex are distributed into multiple extrastriate fields located lateral, anterior, and medial to striate cortex. These fields represent projections to separate visual areas that have been identified with physiological and anatomical methods (Montero, 1973, 1993; Montero et al., 1973a,b; Olavarria and Montero, 1981, 1984, 1989; Espinoza and Thomas, 1983; Thomas and Espinoza, 1987; Coogan and Burkhalter, 1993; Wang and Burkhalter, 2007; Wang et al., 2011).

In rats bilaterally enucleated at birth (BE0), we observed that single, restricted injections of anterogradely transported tracer into striate cortex did not produce diffuse labeling of fibers in extrastriate cortex. Instead, as in normal animals, these injections produced multiple labeled fields that were distributed throughout broad regions of lateral, anterior, and medial extrastriate cortex (Fig. 1B). High-magnification views of fields analyzed in the tangential plane revealed that the borders of extrastriate projection fields in BE0 rats were well defined (Fig. 2B), as in control rats (Fig. 2A). Furthermore, in sections cut in the coronal plane, we observed that labeled fibers in area 18a formed dense, radially oriented, column-like projection fields in both control (Fig. 2C) and BE0 rats (Fig. 2D), and that the laminar distribution of labeled axonal terminations was similar in both groups of animals.

However, striking differences between control and BE0 rats became evident when the overall patterns of area 18a projections were compared. In what follows we will focus our attention to the effect of enucleation on the projections to lateral extrastriate cortex. Figure 3A shows thresholded versions of the projection patterns from five control rats, while Figure 3B shows the patterns from five BE0 rats (the cases shown first in Fig. 3A,B correspond to those shown in Fig. 1A,B, respectively). The thin line within area 17 delineates the injection sites, while the thin line in lateral extrastriate cortex indicates the lateral border of area 18a. The black patches represent the resulting labeled projection fields in area 18a. In order to facilitate the comparison of the patterns shown in Figure 3, the patterns were scaled so that the profile of area 17 in each case matched the profile of area 17 in the first case shown in Figure 3A as closely as possible. Particular attention was paid to matching the size of area 17 along its anteroposterior axis. In agreement with previous studies, we found in normal rats that virtually all projection fields fell within area 18a as defined in Materials and Methods (Figs. 3A, 4I, 5D). In addition, the pattern of 17–18a projections in control rats was remarkably constant from animal to animal, and projections to lateral areas LI and LL were nearly always smaller than projections fields to more medial areas AL, LM, and PL. Moreover, comparing data from animals with injections in different loci within striate cortex (Fig. 4B,C) illustrates that changes in the location of the injection site in striate cortex

produced relatively small displacements of the extrastriate projection fields, and that these displacements were in accord with the topography of the extrastriate visual areas (Olavarria and Montero, 1984; Coogan and Burkhalter, 1993; Montero, 1993). For instance, Figure 4B illustrates that projection fields in areas AL and LM tend to fuse when injections are placed anteriorly in area 17, but they separate in the anteroposterior axis when the injections move posteriorly. Likewise, Figure 4C illustrates that the maps in lateral visual areas mirror the topography in V1, i.e., projection fields in most areas translocate medially as the injection site moves from medial to lateral within area 17.

In BE0 rats, as in control rats, projection fields from restricted loci in area 17 were largely restricted to area 18a as defined in Materials and Methods (Figs. 3B, 4J, 5E,F). However, projection fields within area 18a were not arranged into medial and lateral tiers as clearly as in controls, and fields removed from the 17/18a border were not always smaller than fields close to this border. Also in marked contrast to controls, the patterns of 17–18a projections in BE0 rats were very variable from animal to animal, and it was typically not possible to transform the pattern in one animal into that of another simply by displacing the fields in a consistent manner, as is often the case in normal animals. For instance, Figure 4D illustrates a displacement of injection sites along the anteroposterior axis. However, unlike Figure 4B, the projection patterns resulting from each injection in Figure 4D are very different from each other, with no simple way of transforming one pattern into the other. Moreover, Figure 4E illustrates that projection patterns can be very different even if they originate from injections placed at similar locations in different animals. These observations suggest that the variability in the overall pattern of 17–18a projections in BE0 rats is not primarily due to changes in the location of the injection sites.

To gain further appreciation of the variability in the overall spatial distribution of the patterns of striate–extrastriate projections in each of the four experimental groups analyzed, the thresholded patterns in each group shown in Figure 3 were merged after their orientation had been adjusted so that the lateral border of striate cortex coincided as closely as possible within each group. In addition to using the border of striate cortex identified in the myelin and/or callosal patterns, this adjustment was facilitated by using other landmarks such as the border of area 18a, the location of auditory cortex, and of the barrel field in somatosensory cortex, which were often visible in sections analyzed for myelin or HRP-labeling (Fig. 5). The merged injection sites and striate projection patterns for each group are shown in Figure 4I–L, and for clarity, a single area 17 border representative of all borders in each group was drawn. Inspection of Figure 4J illustrates that the merged striate projection pattern was very different in BE0 animals compared to that in control cases (Fig. 4I). Moreover, the merged pattern in the control group bears a general resemblance to the individual patterns in this group (compare with control cases in Figs. 1, 3), whereas the merged pattern in the BE0 group bears little resemblance to any of the individual patterns in the group (compare with BE0 cases in Figs. 1, 3).

Abnormalities of striate–extrastriate projections correlate with abnormal features of the callosal pattern in lateral extrastriate cortex

In normal rats, previous studies have shown that loci in acallosal regions of striate cortex project virtually exclusively into acallosal islands within extrastriate cortex (Fig. 5D; Olavarria and Montero, 1984; Coogan and Burkhalter, 1993). This correlation suggests that the distributions of both ipsilateral and interhemispheric connections are regulated by a common mechanism. To determine whether enucleation disrupts the correlation between both systems of corticocortical connections, we compared the distributions of striate–extrastriate projections with the pattern of callosal connections revealed in the same animals following multiple injections of HRP in the contralateral hemisphere. As described previously (Olavarria et al., 1987), we observed that while the overall arrangement of

callosal and acallosal regions seen in extrastriate cortex of normal rats is still recognizable in rats enucleated at birth, it is often distorted and highly variable. For instance, bridge-like callosal bands that normally separate the various callosal rings (arrows in Fig. 5A,C) are often interrupted, appearing instead as stumps protruding into acallosal regions at irregular locations (see asterisks in Figs. 5E, 6A,D,G). Sometimes isolated, labeled callosal patches appear in the middle of acallosal regions (indicated by arrows in Fig. 6A,D). We found a striking correlation, illustrated in Figures 5 and 6, between anomalous patterns of striate–extrastriate projections and abnormal features of the callosal pattern. For instance, labeled striate–extrastriate projection fields often extend across gaps in the bridge-like callosal bands, and protrude/invade from one acallosal compartment to another. This is particularly well illustrated in Figure 6D–F. In this case, an extremely long labeled field crosses at least three such gaps, extending uninterruptedly through three acallosal compartments (marked 1–3 in Fig. 6D). In this case it is also interesting to observe that, in acallosal compartment 3, a labeled extension emanating from the long 17–18a projection field wraps around the isolated callosal patch indicated by an arrow (Fig. 6E,F). The case shown in Figure 6A–C also illustrates a protrusion of labeled projections (asterisk) occurring between acallosal compartments 3 and 4, as well as wrapping of labeled 17–18a projections around an isolated callosal patch located in the middle of an acallosal region (indicated with an arrow in Fig. 6A,C). The existence of gaps in the bridge-like callosal bands suggests that enucleation often interferes with the development of the middle portions of the bridges. In some cases, gaps may appear because the callosal protrusions on either side of area 18a become misaligned with each other. The latter is illustrated in Figure 5E, in which asterisks mark two fingerlike protrusions that would have formed a bridge had they developed in alignment with each other. It is interesting to note that a field of labeled striate–extrastriate projections is “wedged” between these two finger-like protrusions (indicated with an arrow in Fig. 5E). This suggests that not only complete callosal bridges, but also callosal protrusions can be associated with separate 17–18a projection fields. This phenomenon may underlie some of the variability in the patterns of projection fields observed among cases enucleated at birth. For example, in normal animals a single acallosal island, associated with visual area anterolateral (AL; Olavarria and Montero, 1984; Montero, 1993; Coogan and Burkhalter, 1993), is typically observed in anterolateral area 18a (see Fig. 5D). As in normal animals, in the enucleated case illustrated in Figure 6A a single acallosal island is visible in this region (marked “2” in Fig. 6A). (The acallosal island marked “1” in Fig. 6A likely corresponds to the anterior callosal ring observed in normal rats, marked with a cross in Fig. 5A,C.) In contrast, in the enucleated case illustrated in Figure 6D–F a callosal protrusion marked with a black asterisk in Figure 6D separates this anterolateral region into two acallosal compartments (marked 2 and 2′ in Fig. 6D), and each of these compartments accommodates separate projection fields (marked with white asterisks in Fig. 6E). The fact that these two projection fields lie within the boundaries of area 18a provides evidence that they represent anomalous projections in the region normally occupied by area AL. Finally, Figure 6D,E illustrates that anomalous projection fields (marked with arrowheads in Figs. 1B, 6E,H) often develop along the 17/18a border, occupying abnormal acallosal islands that are often visible in BE0 rats (marked with arrowheads in Fig. 6D) (Olavarria et al., 1987; Ankaoua and Malach, 1993). In summary, our data show that while neonatal enucleation induces the development of anomalous patterns of striate–extrastriate and callosal connections, it does not significantly degrade the basic correlation observed between these projections in control rats. These results indicate that the mechanisms responsible for this correlation do not depend on retinal input, and suggest that a combination of retinally dependent as well as independent mechanisms is required for the development of normal patterns of striate–extrastriate and callosal connections.

Critical period

To determine the period during which the eyes are critically needed for normal development of striate–extrastriate projections, we studied these projections in animals that were enucleated at P4 (n = 5) or P6 (n = 5). Figure 3C shows the projection pattern in five adult rats enucleated at P4. The first case in Figure 3C is also shown in Figure 1C. Comparison of these patterns with those in normal rats and in rats enucleated at birth suggests that, overall, anomalies in the distribution of projections induced by enucleation at P4 can still be recognized, although they appear less severe than those observed in BE0 rats (cf. Fig. 3C and B). Moreover, Figure 4F illustrates that changes in the projection patterns observed when comparing BE4 cases with injections displaced along the anteroposterior axis do not resemble the changes observed in control animals (cf. Fig. 4B), suggesting that the topography of striate–extrastriate projections is abnormal in BE4 rats. We also examined the pattern of callosal connections in extrastriate cortex of BE4 rats and observed that gaps in the callosal bridges are less prevalent and not as obvious as in BE0 rats. Figure 6I shows relatively small gaps in some callosal bridges, and a large callosal patch that seems to be roughly in the position of the callosal patches indicated by arrows in Figure 6A,D. These observations are consistent with our data from normal and BE0 rats showing that the patterns of striate–extrastriate projections correlate closely with the pattern of callosal connections. Figures 1D and 3D illustrate the striate–extrastriate patterns of projections in five rats enucleated at P6 (the first case in Fig. 3D is also shown in Fig. 1D). These projection patterns appear very similar to those in normally reared rats (cf. Figs. 1D, 1A and 3D, 3A), suggesting that the period during which binocular enucleation disrupts the development of striate–extrastriate projections ends around 6 days of age. Consistent with these observations, comparison of data from animals with injections in different loci within striate cortex (Fig. 4G,H) reveals that, as in control animals (Fig. 4B,C), changes in the location of the injection site in striate cortex produced relatively small displacements of the extrastriate projection fields, and that these displacements were in accord with the topography of the extrastriate visual areas (Olavarria and Montero, 1984; Coogan and Burkhalter, 1993; Montero, 1993). For instance, Figure 4G illustrates that projections fields in areas AL and LM separate from each other along the anteroposterior axis when the injection is placed in posterior area 17, but they tend to approach each other as the injection moves anteriorly. Also, as in Figure 4C, Figure 4H illustrates that the maps in lateral visual areas mirror the topography in V1, i.e., projection fields in most areas translocate medially as the injection site moves from medial to lateral within area 17. Moreover, Figure 4K illustrates that the variability in the striate–extrastriate projection patterns appears reduced in BE4 rats compared to BE0 rats (cf. Fig. 4J), while the variability of the patterns in BE6 rats (Fig. 4L) appears comparable to that observed in control rats (cf. 4I).

Feedforward vs. feedback striate–extrastriate pathways

Previous studies in the rat have shown that the distribution of striate–extrastriate feedforward projections closely matches that of feedback projections (Olavarria and Montero, 1981). To compare the effects of enucleation on the distribution and critical period of feedforward and feedback pathways, in some animals we injected striate cortex with both BDA and a retrogradely transported fluorescent tracer. Figure 7A compares the distributions of retrogradely labeled cells (gray dots) and of anterogradely BDA-labeled projection fields (black areas) in lateral extrastriate cortex following closely placed injections of BDA (large black dot) and red latex fluorescent beads (RB, large gray dot) into striate cortex of a BE0 rat. This diagram illustrates that retrogradely labeled cells tend to accumulate in regions targeted by feedforward projections, and that the overall distribution of feedback projections closely resembles that of feedforward projections. Data from this and two additional cases provide evidence that enucleation at birth has similar effects on both feedforward and feedback pathways. We also compared the distributions of feedback connections in rats

enucleated at P6 with the distribution of feedforward projections in order to determine whether the age at which the eyes are no longer necessary for normal development of feedback projections differs from P6. Data from two animals enucleated at P6 (Fig. 7B,C) show that retrogradely labeled cells (gray dots) accumulate in clusters whose number and general distribution resembles those of anterogradely, BDA-labeled projections (black areas). Moreover, these clusters of labeled cells are displaced with respect to the fields of feedforward projections in a way that is consistent with the topography of extrastriate visual areas in normal rats and mice (Montero, 1973, 1993; Montero et al., 1973a,b; Olavarria and Montero, 1984, 1989; Thomas and Espinoza, 1987; Coogan and Burkhalter, 1993; Wang and Burkhalter, 2007). For example, Figure 7B illustrates that a displacement of the injection site from anterior (BDA, large black dot) to posterior (RB, large gray dot) causes the clusters of labeled cells to displace anteriorly in visual areas AL and PL, but posteriorly in area LM with respect to the feedforward projection fields, as would be expected in normal rats. In Figure 7C, a displacement of the injection sites from medial (BDA, large black dot) to lateral (RB, large gray dot) causes the clusters of labeled cells to displace medially in visual areas AL, LM, and PL, in accord with these areas' normal maps, which mirror the map in V1 in the mediolateral direction (cf. Fig. 4C; Olavarria and Montero, 1984; Thomas and Espinoza, 1987; Montero, 1993; Coogan and Burkhalter, 1993; Wang and Burkhalter, 2007; Wang et al., 2011). Results from these and an additional case (not shown) provide evidence that enucleation at P6 does not prevent the development of normal patterns of feedback connections.

Development of striate–extrastriate projections in neonatally enucleated rats

In newborn rats, parental axons originating in striate cortex and navigating laterally in white matter give off interstitial branches that begin invading gray matter in lateral extrastriate cortex a few days after birth. By P6, many fibers of simple architecture reach the newly formed supragranular cortical layers, and by P8 fibers labeled anterogradely from restricted injections into striate cortex form projection fields that, although sparse, appear to be as well-defined as those observed in adult rats (Ruthazer et al., 2010). To determine whether enucleation at birth changes the time course and definition of the initial invasion of striate–extrastriate projections, we made restricted injections of BDA into striate cortex of BE0 pups at P4 and P6 and analyzed the distribution of anterogradely labeled fibers in lateral striate cortex at P6 and P8, respectively. As in normal pups, parental axons in BE0 animals labeled by the injection of BDA navigate toward area 18a predominantly through deep cortical layers and white matter. Figure 8A illustrates that, as in normal rats, many fibers of simple architecture reach upper layers of the cortex by P6. Moreover, in subsequent days the invasion of additional fibers is not diffuse; instead, invading fibers, many of which are developing terminal arborization patterns, form focused fields (Fig. 8B) whose columnar appearance in coronal sections resembles that of mature projection fields, although the latter appear denser (Fig. 2D). These data provide evidence that neonatal binocular enucleation does not induce obvious changes in the time course of the initial invasion of axon fibers into gray matter, and that, as in normal rats, invading fibers form focused projection fields from the beginning of the invasion.

Quantitative analysis

Our qualitative analysis presented above provides evidence that neonatal enucleation induces the development of abnormal and highly variable patterns of striate–extrastriate projections, and that these effects are no longer obvious when enucleation is delayed until P6. We also analyzed our data quantitatively to investigate whether or not enucleation compromises the relationship between the overall size of the projection in area 18a and the size of the injection sites in striate cortex. In normal animals, the existence of topographically organized striate–extrastriate projections implies that the size of the

projections in area 18a with respect to the size of area 18a increases in proportion to the increase in the size of the injection sites with respect to the size of area 17. If this rule were compromised by enucleation, it could lead to a reduction, or even lack of topography in striate–extrastriate projections. To investigate this possibility it was necessary to determine the effects of enucleation on the sizes of area 17 and 18a, and to measure the sizes of the injection sites and of the projection fields in area 18a of control and enucleated animals (see Materials and Methods). We found that the size of striate cortex measured from tangential sections was significantly larger ($P < 0.05$) in control rats (M = 14.89 mm^2, SD = 0.95, n = 6; see also Olavarria et al., 1987) compared to BE0 (M = 9.08 mm^2, SD = 1.3, n = 6), BE4 (M = 10.63 mm^2, SD = 1.18, n = 5) and BE6 (M = 12.49 mm^2, SD = 0.72, n = 5) rats (Fig. 9A). Expressed as percent of the size of area 17 in control rats, on average the size of area 17 was 61%, 71.4%, and 83.95% in BE0, BE4, and BE6 rats, respectively. Figure 9A also shows that while enucleation performed at later ages had less effect on the size of area 17, the size of area 17 in rats enucleated at P6 was still significantly smaller than that in control rats. In agreement with a recent study in the ferret (Bock et al., 2012), these results indicate that the critical period for the effect of enucleation on the size of area 17 extends beyond the critical period for the effect of enucleation on the pattern of corticocortical projections. In sharp contrast to the effects of enucleation on the size of area 17, we found that area 18a, as defined in Materials and Methods (Fig. 4A), was not significantly larger ($P < 0.05$) in controls (M = 9.70 mm^2, SD = 0.45) compared to BE0 (M = 8.91 mm^2, SD = 1.39), BE4 (M = 9.05 mm^2, SD = 1.18) and BE6 rats (M = 8.79 mm^2, SD = 0.50) rats (Fig. 9A). Figure 9B, which plots the ratio between the sizes of areas 18a and area 17, shows that in normal rats area 18a is about 65% of the size of area 17, while in BE0 rats, due to the nearly 39% reduction in the size of area 17, the size of area 18a approximates (98%) the size of area 17. Thus, as illustrated in Figure 10B, area 17 projects to a target area that is relatively much larger in BE0 than in control rats. Does this significant increase in the size of area 18a relative to the size of area 17 in BE0 rats alter the normal relationship between the size of the projections in area 18a and the size of the injections into area 17? To answer this question, we calculated the ratio between the fraction of area 18a occupied by the overall size of the projection and the fraction of area 17 occupied by the injection site in control and enucleated rats. This ratio was not significantly different ($P < 0.05$) between control rats (1.5, SD = 0.24) and any of the enucleated groups of rats (BE0 = 1.6, SD = 0.44; BE4 = 1.4, SD = 0.39; BE6 = 1.38, SD = 0.31). Moreover, as shown in the scatterplot in Figure 9C, the data from all four groups could be fit by a regression line ($r^2 = 0.78$) with slope = 1.46 (formula: Y = 1.46X + 0.004). These results therefore indicate that early enucleation does not alter the normal relationship that exists between the relative sizes of the projection fields in area 18a and the relative sizes of the injection sites in area 17. These results further suggest that altering this relationship is not necessary for the development of anomalous topographic projections in enucleated animals. Moreover, as illustrated in the diagram of Figure 10, these data suggest that maintenance of this proportionality in enucleated animals is achieved through a corresponding increase in the divergence of projections from area 17 to area 18a, i.e., an increase in the ratio between the overall size of the projection in 18a and the size of the tracer injection in area 17. For example, Figure 10 illustrates that a tracer injection that occupies, for instance, 10% of area 17 in control rats (Fig. 10A) would occupy ≈16.4% of area 17 in BE0 rats (Fig. 10B) due of the reduction in the size of this area observed in these animals (Fig. 9A). From the correlation shown in Figure 9C it follows that the proportion of area 18a occupied by the resulting projections would be correspondingly greater in BE0 rats than in control rats. However, because area 18a is approximately the same size in both control and BE0 rats (Fig. 9A), the absolute size of the 18a projection produced by an injection of the same size would be greater in BE0 than in control rats (cf. Fig. 10A,B). Indeed, we found that the ratio between the overall size of the projection in area 18a and the size of the injection site in area 17 was significantly larger ($P < 0.05$) in

BE0 rats (M = 1.69, SD = 0.6) compared to control rats (M = 0.97, SD = 0.15), confirming that enucleation causes an increase in the divergence of striate-extrastriate projections.

Discussion

Studies from several laboratories have shown that the pattern of striate-extrastriate projections in the rat is remarkably consistent from animal to animal (Olavarria and Montero, 1984; Malach, 1989; Montero, 1993; Coogan and Burkhalter, 1993). Moreover, these studies showed that tracer injections into different regions of V1 produce essentially the same projection patterns, except that the projection fields translocate locally according to the retinotopic organization of extrastriate visual areas. In contrast, in the present study we found that bilateral enucleation at birth leads to the development of striate-extrastriate projections patterns that are highly anomalous and variable from animal to animal. Unlike control rats, it was often not possible to transform the patterns observed in different rats by displacing the overall set of projection fields. A highly variable pattern of cortical projections to area 17 has also been described in neonatally enucleated opossums (Karlen et al., 2006). As in this previous study, the variability we observed does not seem to be due to differences in the location of injection sites because animals with injections in similar locations often showed widely different projection patterns. If extrastriate cortex in BE0 rats were subdivided into multiple striate-recipient areas, our observations would suggest that, unlike normal rats, the arrangement of these areas would vary considerably among animals. Our results are in agreement with a previous study describing anomalous striate–extrastriate projections in both neonatally enucleated and anophthalmic rats (Bravo and Inzunza, 1994), and are consistent with experiments in hamsters (Kingsbury et al., 2002) and cats (Carić and Price, 1999) showing that early ablation of thalamic input leads to abnormal corticocortical connections. Moreover, our data from animals injected with both anterogradely and retrogradely transported tracers into striate cortex showed that enucleation at birth induces similar anomalies on both feedforward and feedback pathways. These results provide evidence that the development of normal striate–extrastriate connections depends critically on retinal influences.

Our quantitative analysis revealed that the size of area 17, but not that of area 18a, is markedly smaller in early enucleates compared to controls, leading to a pronounced mismatch between the sizes of area 17 and 18a. This mismatch is compensated by an increase in the divergence of striate–extrastriate projections, which prevents enucleation from altering the normal relationship that exists between the proportion of area 18a occupied by the projection from area 17, and the proportion of area 17 occupied by the tracer injection. In order to calculate the relationship between the relative sizes of the projection fields in area 18a and the relative sizes of the injection sites in area 17, it was necessary that we measure the sizes of areas 17, 18a, the overall projection in area 18a, and the size of the tracer injections. Our measurements of the size of area 17 are likely accurate because they are based on the profile of area 17 as revealed by myelin and callosal patterns in tangential sections of the flattened cortex. In addition, they are in good agreement with previous estimates of the size of area 17 (Olavarria et al., 1987). Likewise, we believe that our measurements of the overall size of the projection in area 18a are accurate because they are based on BDA-staining patterns that could be readily scanned and processed by imaging programs. However, although the lateral border of area 18a can be readily recognized from myelin and callosal patterns, there are no clear criteria for recognizing the anterior border of this area. In order to compare the size of area 18a across all experimental groups, we traced the anterior border of area 18a using common landmarks identifiable in all animals, but which were somewhat arbitrary (see Materials and Methods). It is therefore possible that we underestimated the size of area 18a. Similarly, we estimated the sizes of the injection sites using two approaches that were highly consistent with each other, but it is possible that the

sizes we measured do not correspond to that of the effective injection sites. As explained in Materials and Methods, striate projections to the superior colliculus or lateral geniculate nucleus could not be used to compare the effective injection site between control and enucleated animals because striate-subcortical connections are abnormal in neonatally enucleated rodents (e.g., Warton et al., 1988). However, since the same procedures were used to measure the size of the tracer injections and area 18a in all experimental groups, potential differences between our measurements and the actual sizes of area 18a and of the effective tracer injections would not necessarily invalidate our comparative analysis across groups.

The increase in the divergence of striate–extrastriate projections that we observed in early enucleated rats is consistent with a recent study reporting that neonatal enucleation increases the divergence/convergence of callosal connections in rat visual cortex (Bock and Olavarria, 2011), which raises the possibility that increases in the divergence/convergence of connections is a common plastic response to early deafferentation in the central nervous system. It is also interesting to note that our finding that area 17, but not area 18a, is reduced in enucleated rats contrasts with a recent report that early enucleation in the ferret is associated with a reduction in the size of both striate and extrastriate visual areas (Bock et al., 2012). Projections from the dLGN have been implicated in the regulation of the size of visual areas (see Bock et al., 2012, for references relevant to this issue). In this context, the difference between our results in the rats and those reported in the ferret is probably related to the fact that projections from the dLGN are largely restricted to area 17 in the rat (Ribak and Peters, 1975; Schober and Winkelmann, 1977; Olavarria, 1979), while in the ferret, in addition to area 17, direct retinogeniculate projections also innervate area 18 and possibly other extrastriate visual areas (Redies et al., 1990; Ruthazer et al., 1999; White et al., 1999; Innocenti et al., 2002).

Retinal influences specify normal patterns of striate–extrastriate connections by P6

Our data from delayed enucleations show that the patterns of 17–18a projections appear less disrupted when enucleation is performed at P4 than when enucleation is performed at P0. However, delaying enucleation by only 2 more days results in 17–18a projection patterns that closely resemble the patterns in control animals. Our data show that the patterns of projections in adult rats enucleated at P6 are very similar to the patterns in control rats in the overall arrangement and relative location of the projection fields, as well as in the consistency of the overall pattern from animal to animal. Moreover, we showed that the feedback projection from lateral extrastriate cortex to striate cortex also appears immune to enucleation by P6. These results indicate that retinal input ceases to influence the development of feedforward and feedback striate–extrastriate projections by P6. Previous studies have reported that both binocular and monocular neonatal enucleation alter the overall distribution of callosal connections in the 17/18a callosal zone of rats and mice (Cusick and Lund, 1982; Olavarria and Van Sluyters, 1984; Olavarria et al., 1987). Moreover, the appearance of the overall visual callosal pattern (Olavarria et al., 1987), as well as its point-to-point topography (Olavarria and Hiroi, 2003), abruptly becomes immune to the effects of eye removal at P6. Thus, our present results together with those from previous studies of the callosal pathway indicate that the overall distributions of callosal connections and ipsilateral striate–extrastriate connections become specified at about the same time during early stages of development, possibly by similar retinally driven mechanisms. If these mechanisms depended on ganglion cell activity, the likely source would be spontaneous activity because the eyes open by P13, ruling out a role for visual experience in the development of striate–extrastriate projection patterns. Although enucleation at P6 did not have an obvious effect on the patterns of striate–extrastriate connections, it still had a significant effect on the size of striate cortex. Similar observations

have been reported in a recent study of the effects of neonatal enucleation on the pattern of callosal connections and the size of visual areas in the ferret (Bock et al., 2012). These observations suggest that retinal influences regulate several aspects of cortical development through mechanisms that do not necessarily operate during the same time window. Moreover, they indicate that the pattern of visual corticocortical connections can develop without obvious abnormalities even if the size of striate cortex is somewhat smaller than normal.

At first sight, our results that the critical period for the feedback pathway coincides with that for the feedforward pathway may seem at odds with reports that development of feedback pathways in humans (Burkhalter, 1993) and mice (Dong et al., 2004) is delayed by several days when compared to that for the feedforward pathway. Assuming that the development of the feedback pathway is also delayed in normal rats, our finding of a common critical period for both pathways suggests that the timing of the critical period for the effect of the eyes does not primarily depend on the timing of axon arrival at the target region. For example, during the critical period, chemical cues induced by retinally driven processes could lay down a “blueprint” for normal patterns of feedforward and feedback projections. In this scenario, fibers from extrastriate cortex would still be able to “read” the instructions in the blueprint even if they arrive at their targets with some delay. In the present study we found that the development of feedforward striate–extrastriate projections in neonatally enucleated rats proceeds with a time course that is similar to that of feedforward projections in normal-eyed animals (Ruthazer et al., 2010). If in normal rats the development of the feedback projection were delayed relative to the development of feedforward projections, as it is in humans (Burkhalter, 1993) and mice (Dong et al., 2004), it would be of interest to determine whether the time course for the development of the feedback projection is similarly delayed in neonatally enucleated rats. Finding that this is indeed the case would provide further evidence that the timing of axon growth and invasion of gray matter for different pathways is likely triggered by mechanisms depending on central, rather than retinal, factors.

Role of retinal input on the development of striate–extrastriate projection patterns

A recent study of the development of the 17–18a projection in normal rat pups found that axonal interstitial branches of simple architecture reach superficial layers by P6, and that by P8 fibers originating from a single, small injection of BDA in area 17 formed well-defined, focused projection fields at the correct topographical locations in area 18a (Ruthazer et al., 2010). In the present study we observed that striate–extrastriate projections in pups enucleated at birth also reach superficial cortical layers by P6, providing evidence that the timing of fiber invasion and growth in area 18a is independent from retinal influences. A similar schedule for fiber invasion and growth in gray matter has been reported for visual callosal connections in both normal rats and in rats enucleated at birth (Olavarria and Safaeian, 2006). Moreover, as in normal pups (Ruthazer et al., 2010), our data from pups enucleated at birth and studied at P6 or P8 show that fibers invading area 18a from area 17 form well-defined projection fields from the beginning of the invasion, suggesting that the highly variable projection patterns observed in area 18a of mature neonatally enucleated rats do not result from anomalous pruning of exuberant distributions of 17–18a fibers in gray matter. These results in young enucleated pups, together with our finding that lack of retinal influences during the critical period results in highly variable patterns of striate–extrastriate connections in adult rats suggest that retinal influences regulate the spatial arrangement of striate–extrastriate projection patterns, but not the timing and definition of the initial invasion of area 18a by striate projection axons.

What may account for the high variability of striate–extrastriate projections observed in neonatally enucleated rats? Ruthazer et al. (2010) also performed a time-lapse analysis of the development of 17–18a projections in normal pups and reported that many

filopodiumlike branches emerged along parental axons in white matter or deep layers in area 18a. Most of these filopodial branches were transient, often disappearing after several minutes to hours of exploratory extension and retraction. On the basis of their fixed tissue and time-lapse observations, Ruthazer et al. (2010) proposed that the development of topographically organized corticocortical projections in rats involves extensive exploratory branching along parental axons and invasion of cortex by only a small number of interstitial branches which grow toward the pia at topographically correct places. Ruthazer at al. (2010) further suggested that the growth of branches at topographically correct places could be specified both by a combination of local mapping cues, such as the graded expression patterns of ephrinA (Cang et al., 2005), and cues from the eyes, either in the form of patterned neural activity (Ruthazer et al., 2003; Cang et al., 2008) or thalamic afferent-derived molecular signals (Sugiyama et al., 2008). The observation that small, dynamic filopodiumlike branches also emerge from 17–18a parental axons in neonatally enucleated rats (E. Ruthazer and J. Olavarria, unpubl. obs.), together with our present data from BDA-labeled fibers in neonatal rats, suggest that striate–extrastriate projections go through similar developmental stages in both control and enucleated rats, except that the arrangement and topography of the projections are anomalous in enucleated rats. This lack of topography could result from the loss of retinal topographic cues caused by enucleation, which would leave only local cues in charge of specifying the places along the parental axons where small dynamic branches are to grow toward the pia. It is possible that the spatial distribution of these local cues varies significantly from animal to animal, leading to the development of highly variable patterns of striate–extrastriate projections in enucleated animals.

Callosal to callosal, acallosal to acallosal rule

In normal rats, callosal connections occupy approximately the lateral third of area 17, while in area 18a they form more or less continuous bands on either side of the area, as well as a series of callosal bridges dividing area 18a in a number of compartments that correspond closely to visual areas described physiologically (Fig. 5A,C,D). Previous studies (Olavarria and Montero, 1984; Coogan and Burkhalter, 1993; Ankaoua and Malach, 1993), as well as our present results illustrate that projections from area 17 to ipsilateral area 18a obey the general rule “callosal to callosal, acallosal to acallosal,” i.e., medial, acallosal regions of area 17a project to acallosal islands in area 18a, while the lateral, callosal region of area 17 projects to callosal regions located preferentially at the border of visual areas in lateral extrastriate cortex. In normal rats, this rule likely reflects the fact that projections from restricted loci in striate cortex are distributed according to the topography of extrastriate visual areas identified physiologically (Montero, 1973; Montero et al., 1973b; Thomas and Espinoza, 1987). Thus, the lateral, callosal region in area 17 represents portions of the visual field located close to, or on the vertical meridian of the visual field, and this region projects to the medial, as well as other callosal regions in ipsilateral area 18a, which represent the same central regions of the visual field. Similarly, medial, acallosal regions in area 17 represent more peripheral portions of the visual field, and they project to acallosal islands in ipsilateral area 18a, which also represent peripheral fields. In the present report we focused our attention on the projections from medial, acallosal regions of area 17 to highlight the close complementarity of these projections with the pattern of callosal connections in area 18a (Fig. 5C,D), and to examine whether this relationship is affected by the removal of topographic cues from retinal origin. Our results indicate that enucleation leads to the development of anomalous striate–extrastriate and callosal connections. However, the abnormalities in 17–18a projections mirror the abnormalities in the callosal pattern in such a way that projections from medial, acallosal regions of striate cortex remain confined to acallosal territories in area 18a, thereby maintaining the complementarity between these pathways that is observed in normal animals. These results indicate that this complementarity does not depend on topographic cues from the retina, and provide evidence

that, in spite of abnormalities in the topography of striate–extrastriate projections, the rule "callosal to callosal, acallosal to acallosal" remains valid in neonatally enucleated rats. Mechanisms underlying this complementary may relate to central cues specifying the distribution of callosal and noncallosal territories, and several scenarios are possible. For instance, callosal and noncallosal territories may be "marked" by cues that attract projections from callosal and noncallosal territories, respectively. Alternatively, callosal and noncallosal territories may be specified by cues that are mutually repulsive. In this case, projections originating from acallosal regions in area 17 would be confined to acallosal territories in area 18a because callosal regions in areas 17 and 18a would repel them. A similar mechanism would restrict projections originating from callosal regions in area 17 to callosal territories in area 18a. However, these mechanisms require that both pathways be specified by specific markers, making it hard to explain how the distribution of separate markers would vary in tandem to induce variability in the distribution of striate–extrastriate and callosal connections without loss of complementarity. Perhaps central cues only specify the territory for one of these pathways, which would then act as a template to passively mold the distribution of the other one through repellent interactions. This would allow variability in the template without loss of complementarity. The cues involved are not known at present, but they may be similar to guidance labels that have been implicated in the establishment of topographically organized thalamocortical projections. For instance, Cang et al. (2005) showed that EphA/ephrin-A interactions are involved at central levels of the visual pathway, including primary visual cortex, and suggested that they may have a role in mapping projections from primary to nonprimary visual areas. Further research is necessary to determine the mechanisms regulating the patterns of striate–extrastriate and callosal connections, and how they give rise to ensembles of topographically organized visual areas that are highly constant from animal to animal. Our data suggest that retinal input may not only specify the normal arrangement of extrastriate visual areas, but also their normal internal topography, a question we are currently investigating in more detail using injections of multiple tracers in the same animal. Finally, studying how striate–extrastriate and callosal connections interact during development may yield important clues toward understanding evolutionary changes in the segmentation and arrangement of cortical visual areas across species.

Acknowledgments

Grant sponsor: National Institutes of Health; Grant number: EY016045 (to J.F.O.); Grant sponsor: Royalty Research Fund Award, University of Washington (to J.F.O.).

Literature Cited

Ankaoua D, Malach R. Evidence for plasticity of intrinsic horizontal connections in area 17 of the rat. Isr J Med Sci. 1993; 29:555–569. [PubMed: 8225945]

Belford GR, Killackey HP. The sensitive period in the development of the trigeminal system of the neonatal rat. J Comp Neurol. 1980; 193:335–350. [PubMed: 7440771]

Bock AS, Olavarria JF. Neonatal enucleation during a critical period reduces the precision of cortico-cortical projections in visual cortex. Neurosci Lett. 2011; 501:152–156. [PubMed: 21782890]

Bock AS, Kroenke CD, Taber EN, Olavarria JF. Retinal input influences the size and cortico-cortical connectivity of visual cortex during postnatal development in the ferret. J Comp Neurol. 2012; 520:914–932. [PubMed: 21830218]

Bravo H, Inzunza O. Effect of pre- and postnatal retinal deprivation on the striate-peristriate cortical connections in the rat. Biol Res. 1994; 27:73–77. [PubMed: 7647817]

Burkhalter A. Development of forward and feedback connections between areas V1 and V2 of human visual cortex. Cereb Cortex. 1993; 3:476–487. [PubMed: 8260814]

Cang J, Kaneko M, Yamada J, Woods G, Stryker MP, Feldheim DA. Ephrin-As guide the formation of functional maps in the visual cortex. Neuron. 2005; 48:577–589. [PubMed: 16301175]

Cang J, Wang L, Stryker MP, Feldheim DA. Roles of ephrin-As and structured activity in the development of functional maps in the superior colliculus. J Neurosci. 2008; 28:11015–11023. [PubMed: 18945909]

Carić D, Price DJ. Evidence that the lateral geniculate nucleus regulates the normal development of visual cortico-cortical projections in the cat. Exp Neurol. 1999; 156:353–362. [PubMed: 10328942]

Caviness VS. Architectonic map of neocortex of the normal mouse. J Comp Neurol. 1975; 164:247–263. [PubMed: 1184785]

Coogan TA, Burkhalter A. Hierarchical organization of areas in rat visual cortex. J Neurosci. 1993; 13:3749–3772. [PubMed: 7690066]

Crowley JC, Katz LC. Early development of ocular dominance columns. Science. 2000; 290:1321–1324. [PubMed: 11082053]

Cusick CG, Lund RD. Modification of visual callosal projections in rats. J Comp Neurol. 1982; 212:385–398. [PubMed: 7161416]

Dehay C, Horsburgh G, Berland M, Killackey H, Kennedy H. Maturation and connectivity of the visual cortex in monkey is altered by prenatal removal of retinal input. Nature. 1989; 337:265–267. [PubMed: 2536139]

Dehay C, Giroud P, Berland M, Killackey H, Kennedy H. Contribution of thalamic input to the specification of cytoarchitectonic cortical fields in the primate: effects of bilateral enucleation in the fetal monkey on the boundaries, dimensions, and gyrification of striate and extrastriate cortex. J Comp Neurol. 1996; 367:70–89. [PubMed: 8867284]

Dong H, Wang Q, Valkova K, Gonchar Y, Burkhalter A. Experience-dependent development of feedforward and feedback circuits between lower and higher areas of mouse visual cortex. Vision Res. 2004; 44:3389–3400. [PubMed: 15536007]

Erzurumlu RS, Killackey HP. Critical and sensitive periods in neurobiology. Curr Top Dev Biol. 1982; 17:207–40. [PubMed: 7140347]

Espinoza SG, Thomas HC. Retinotopic organization of striate and extrastriate visual cortex in the hooded rat. Brain Res. 1983; 272:137–144. [PubMed: 6616189]

Fagiolini M, Pizzorusso T, Berardi N, Domenici L, Maffei L. Functional postnatal development of the rat primary visual cortex and the role of visual experience: dark rearing and monocular deprivation. Vision Res. 1994; 34:709–720. [PubMed: 8160387]

Fish SE, Rhoades RW, Bennett-Clarke CA, Figley B, Mooney RD. Organization, development and enucleation-induced alterations in the visual callosal projection of the hamster: single axon tracing with Phaseolus vulgaris leucoagglutinin and Di-I. Eur J Neurosci. 1991; 3:1255–1270. [PubMed: 12106224]

Godement P, Saillour P, Imbert M. Thalamic afferents to the visual cortex in congenitally anophthalmic mice. Neurosci Lett. 1979; 13:271–278. [PubMed: 530479]

Guillery RW, Ombrellaro M, LaMantia AL. The organization of the lateral geniculate nucleus and of the geniculocortical pathway that develops without retinal afferents. Brain Res. 1985; 352:221–233. [PubMed: 4027668]

Innocenti, GM. Progress in sensory physiology. Berlin: Springer; 1991. The development of projections from cerebral cortex; p. 65-114.

Innocenti GM, Frost DO. The postnatal development of visual callosal connections in the absence of visual experience or of the eyes. Exp Brain Res. 1980; 39:365–375. [PubMed: 7398830]

Innocenti GM, Manger PR, Masiello I, Colin I, Tettoni L. Architecture and callosal connections of visual areas 17, 18, 19 and 21 in the ferret (*Mustela putorius*). Cereb Cortex. 2002; 12:411–422. [PubMed: 11884356]

Kaiserman-Abramof IR, Graybiel AM, Nauta WJ. The thalamic projection to cortical area 17 in a congenitally anophthalmic mouse strain. Neuroscience. 1980; 5:41–52. [PubMed: 7366842]

Karlen SJ, Kahan DM, Krubitzer L. Early blindness results in abnormal and thalamocortical connections. Neuroscience. 2006; 142:843–858. [PubMed: 16934941]

Kingsbury MA, Lettman NA, Finlay BL. Reduction of early thalamic input alters adult corticocortical connectivity. Brain Res Dev Brain Res. 2002; 138:35–43.

Krieg WJS. Connections of the cerebral cortex I. The albino rat. A. Topography of the cortical areas. J Comp Neurol. 1946; 84:221–275. [PubMed: 20982805]

Malach R. Patterns of connections in rat visual visual cortex. J Neurosci. 1989; 9:3741–3752. [PubMed: 2479724]

Maunsell JH. Functional visual streams. Curr Opin Neurobiol. 1992; 2:506–510. [PubMed: 1525550]

Mesulam MM. Tetramethyl benzidine for horseradish peroxidase neurohistochemistry: a non-carcinogenic blue reaction product with superior sensitivity for visualizing neural afferents and efferents. J Histochem Cytochem. 1978; 26:106–117. [PubMed: 24068]

Montero VM. Evoked responses in the rat's visual cortex to contralateral, ipsilateral, and restricted photic stimulation. Brain Res. 1973; 53:192–196. [PubMed: 4572482]

Montero VM. Retinotopy of cortical connections between the striate cortex and extrastriate visual areas in the rat. Exp Brain Res. 1993; 94:1–15. [PubMed: 8335065]

Montero VM, Brugge JF, Beitel RE. Relation of the visual field to the lateral geniculate body of the albino rat. J Neurophysiol. 1968; 31:221–236. [PubMed: 5687382]

Montero VM, Bravo H, Fernández V. Striate-peristriate cortico-cortical connections in the albino and gray rat. Brain Res. 1973a; 53:202–207. [PubMed: 4348900]

Montero VM, Rojas A, Torrealba F. Retinotopic organization of striate and peristriate visual cortex in the albino rat. Brain Res. 1973b; 53:197–201. [PubMed: 4697246]

O'Brien BJ, Olavarria JF. Anomalous patterns of callosal connections develop in visual cortex of monocularly enucleated hamsters. Biol Res. 1995; 28:211–218. [PubMed: 9251751]

Olavarria J. A horseradish peroxidase study of the projections from the latero-posterior nucleus to three lateral peristriate areas in the rat. Brain Res. 1979; 173:137–141. [PubMed: 487075]

Olavarria JF, Hiroi R. Retinal influences specify corticocortical maps by postnatal day six in rats and mice. J Comp Neurol. 2003; 459:156–172. [PubMed: 12640667]

Olavarria JF, Li CP. Effects of neonatal enucleation on the organization of callosal linkages in striate cortex of the rat. J Comp Neurol. 1995; 361:138–151. [PubMed: 8550875]

Olavarria J, Montero VM. Reciprocal connections between the striate cortex and extrastriate cortical visual areas in the rat. Brain Res. 1981; 217:358–363. [PubMed: 7248793]

Olavarria J, Montero VM. Relation of callosal and striate-extrastriate cortical connections in the rat: morphological definition of extrastriate visual areas. Exp Brain Res. 1984; 54:240–252. [PubMed: 6723844]

Olavarria J, Montero VM. Organization of visual cortex in the mouse revealed by correlating callosal and striate-extrastriate connections. Vis Neurosci. 1989; 3:59–69. [PubMed: 2487092]

Olavarria JF, Safaeian P. Development of callosal topography in visual cortex of normal and enucleated rats. J Comp Neurol. 2006; 496:495–512. [PubMed: 16572463]

Olavarria J, Van Sluyters RC. Callosal connections of the posterior neocortex in normal-eyed, congenitally anophthalmic, and neonatally enucleated mice. J Comp Neurol. 1984; 230:249–268. [PubMed: 6512020]

Olavarria J, Van Sluyters RC. Organization and postnatal development of callosal connections in the visual cortex of the rat. J Comp Neurol. 1985; 239:1–26. [PubMed: 4044927]

Olavarria JF, Van Sluyters RC. Overall pattern of callosal connections in visual cortex of normal and enucleated cats. J Comp Neurol. 1995; 363:161–176. [PubMed: 8642068]

Olavarria J, Malach R, Van Sluyters RC. Development of visual callosal connections in neonatally enucleated rats. J Comp Neurol. 1987; 260:321–348. [PubMed: 3597836]

Olavarria J, Bravo H, Ruiz G. The pattern of callosal connections in posterior neocortex of congenitally anophthalmic rats. Anat Embryol (Berl). 1988; 178:155–159. [PubMed: 3134833]

Redies C, Diksic M, Riml H. Functional organization in the ferret visual cortex: a double-label 2-deoxyglucose study. J Neurosci. 1990; 10:2791–2803. [PubMed: 2388088]

Rhoades RW, Dellacroce DD. Neonatal enucleation induces an asymmetric pattern of visual callosal connections in hamsters. Brain Res. 1980; 202:189–195. [PubMed: 7427734]

Ribak CE, Peters A. An autoradiographic study of the projection from the lateral geniculate body of the rat. Brain Res. 1975; 92:341–368. [PubMed: 1174957]

Richter CP, Warner CL. Comparison of Weigert stained sections with unfixed, unstained sections for study of myelin sheaths. Proc Natl Acad Sci U S A. 1974; 71:598–601. [PubMed: 4132530]

Ruthazer ES, Baker GE, Stryker MP. Development and organization of ocular dominance bands in primary visual cortex of the sable ferret. J Comp Neurol. 1999; 407:151–165. [PubMed: 10213088]

Ruthazer ES, Akerman CJ, Cline HT. Control of axon dynamics by correlated activity in vivo. Science. 2003; 301:66–70. [PubMed: 12843386]

Ruthazer ES, Bachleda AR, Olavarria JF. Role of interstitial branching in the development of visual corticocortical connections: a time-lapse and fixed-tissue analysis. J Comp Neurol. 2010; 518:4963–4979. [PubMed: 21031561]

Schober W, Winkelmann. Die geniculo-kortikale Projektion bei Albinoratten. J Hirnforsch. 1977; 18:1–20. [PubMed: 894013]

Simon DK, O'Leary DD. Development of topographic order in the mammalian retinocollicular projection. J Neurosci. 1992; 12:1212–1232. [PubMed: 1313491]

Sugiyama S, Di Nardo AA, Aizawa S, Matsuo I, Volvovitch M, Prochiantz A, Hensch TK. Experience-dependent transfer of Otx2 homeoprotein into the visual cortex activates postnatal plasticity. Cell. 2008; 134:508–520. [PubMed: 18692473]

Thomas HC, Espinoza SG. Relationships between interhemispheric cortical connections and visual areas in hooded rats. Brain Res. 1987; 417:214–224. [PubMed: 3651812]

Van Essen DC, Maunsell JHR. Hierarchical organization and functional streams in the visual cortex. Trends Neurosci. 1983; 6:370–375.

Wang Q, Burkhalter A. Area map of mouse visual cortex. J Comp Neurol. 2007; 502:339–357. [PubMed: 17366604]

Wang Q, Gao E, Burkhalter A. Gateways of ventral and dorsal streams in mouse visual cortex. J Neurosci. 2011; 31:1905–1918. [PubMed: 21289200]

Warton SS, Dyson SE, Harvey AR. Visual thalamocortical projections in normal and enucleated rats: HRP and fluorescent dye studies. Exp Neurol. 1988; 100:23–39. [PubMed: 3350091]

White LE, Bosking WH, Williams SM, Fitzpatrick D. Maps of central visual space in ferret V1 and V2 lack matching inputs from the two eyes. J Neurosci. 1999; 19:7089–7099. [PubMed: 10436063]

Zilles, K.; Wree, A. Cortex: areal and laminar structure. In: Paxinos, G., editor. The rat nervous system. San Diego: Academic Press; 1995. p. 649-685.

Zilles K, Zilles B, Schleicher A. A quantitative approach to cytiarchitectonics. Anat Embryol. 1980; 159:335–360. [PubMed: 6970009]

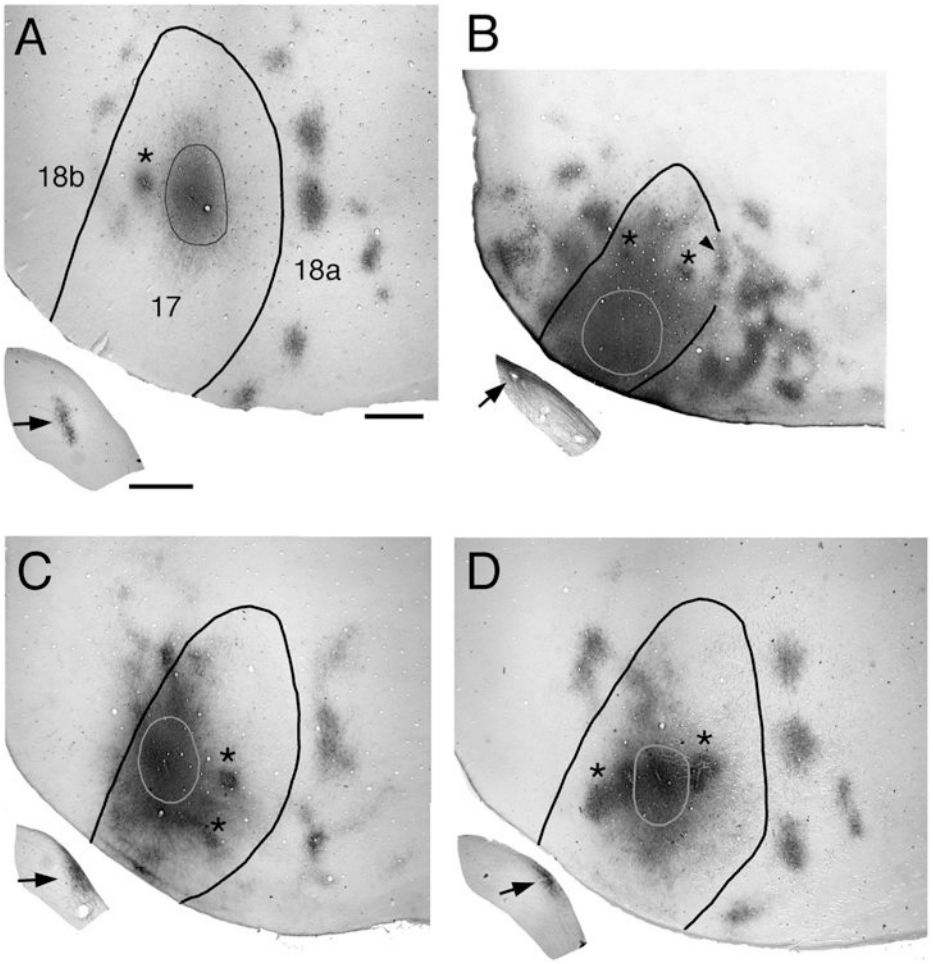

Figure 1.

Effect of bilateral enucleation at different postnatal ages on the pattern of striate–extrastriate projections. Photographs of tangential tissue sections cut through the flattened occipital cortex illustrate the anterogradely labeled projection patterns in extrastriate cortex (areas 18a and 18b; Krieg, 1946; Caviness, 1975) resulting from a single injection of BDA into medial, acallosal regions of striate cortex (area 17). Lateral is to the right, anterior is up. Outlines inside area 17 indicate the injections of the tracer BDA. Asterisks indicate artifactual staining produced by injections of fluorescent tracers. Black arrows in insets indicate the patterns of anterogradely transported BDA labeling in the ipsilateral dLGN. **A:** Control animal. **B:** Enucleation at postnatal day 0 (BE0). Arrowhead indicates labeling at the 17/18a border. **C:** Enucleation at postnatal day 4 (BE4). **D:** Enucleation at postnatal day 6 (BE6). Scale for flattened tissue = 1.0 mm; scale for dLGn = 0.5 mm.

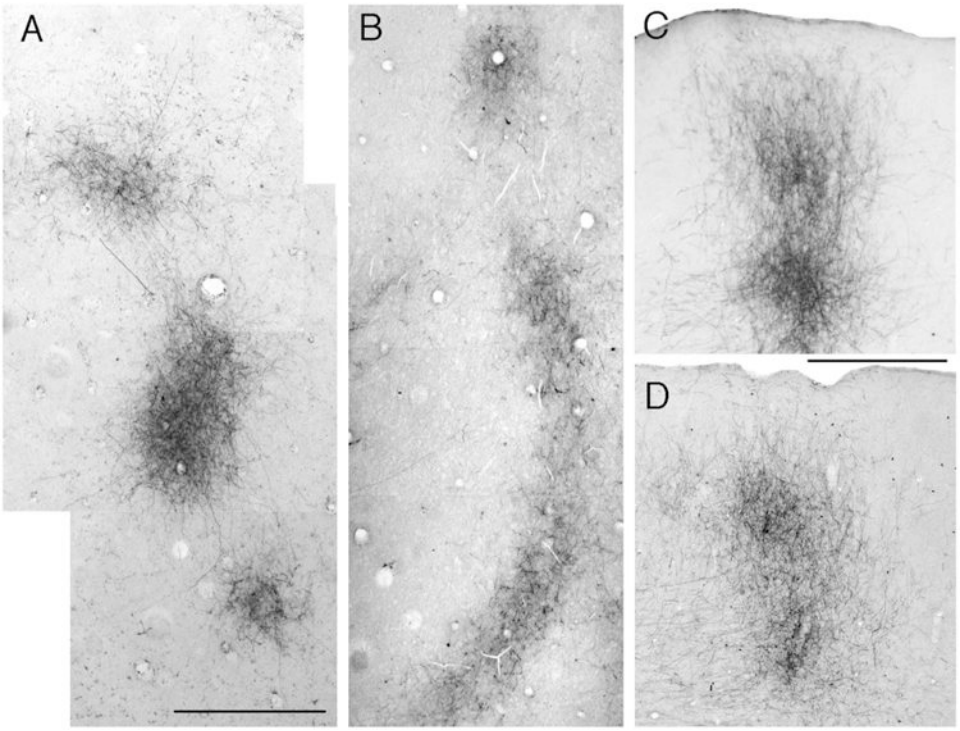

Figure 2.

Effect of bilateral enucleation at birth (BE0) on projections from striate cortex to lateral extrastriate cortex. High-magnification photographs of striate projection fields observed after single injections of BDA into medial, acallosal regions of striate cortex. **A,B:** Projections fields revealed in tangential sections in control (A) and BE0 (B) animals. Lateral is to the right, anterior is up. **C,D:** Projections fields revealed in coronal sections through lateral extrastriate cortex in a control (C) and a BE0 (D) animal. Lateral is to the right. Scale bars = 1.0 mm in A (applies to B); 0.5 mm in C (applies to D).

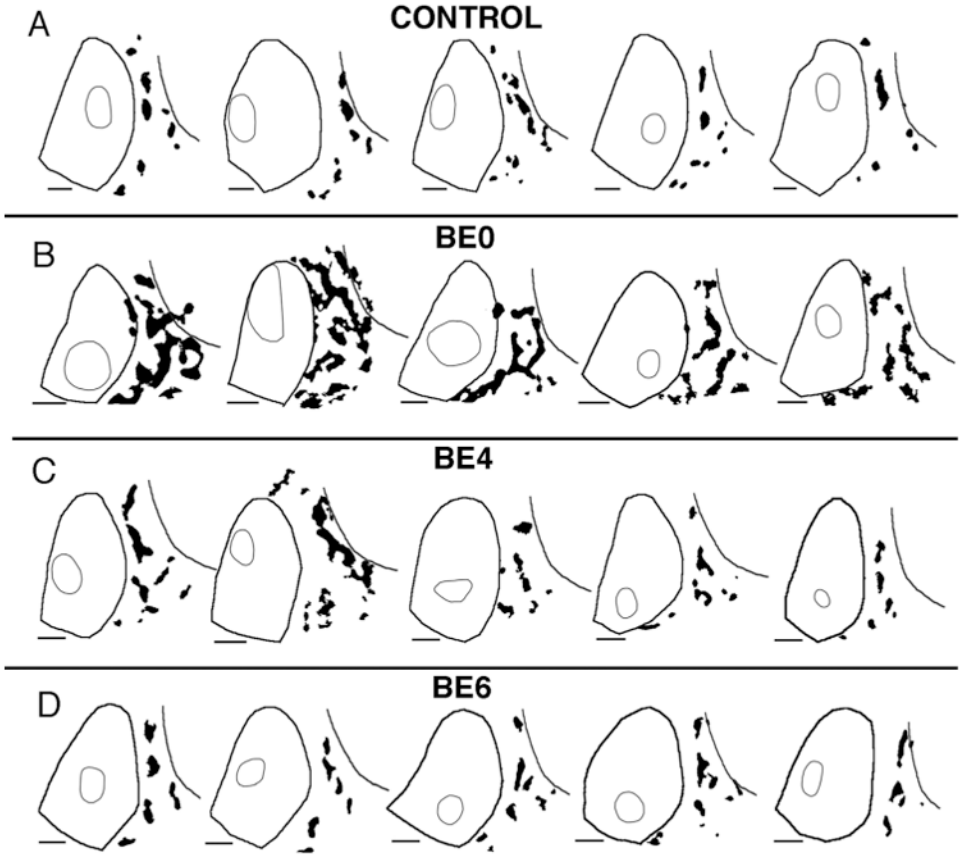

Figure 3.

Patterns of BDA-labeled projections from striate cortex to area 18a in control rats and in rats enucleated at different ages. Lateral is to the right, anterior is up. Thresholded versions of the projection patterns are represented in black. Thick lines delineate the borders of areas 17 and the lateral border of area 18a, while thin outlines outline the BDA injection sites. The injection outlines were drawn at the perimeter where an abrupt transition in the labeling density was observed (see Materials and Methods). The patterns were scaled so that the profile of area 17 in each case matched the profile of area 17 in the first case shown in A as closely as possible. **A:** Control rats. **B:** Rats enucleated at birth (BE0). **C:** Rats enucleated at postnatal day 4 (BE4). **D:** Rats enucleated at postnatal day 6 (BE6). Scale bars = 1.0 mm.

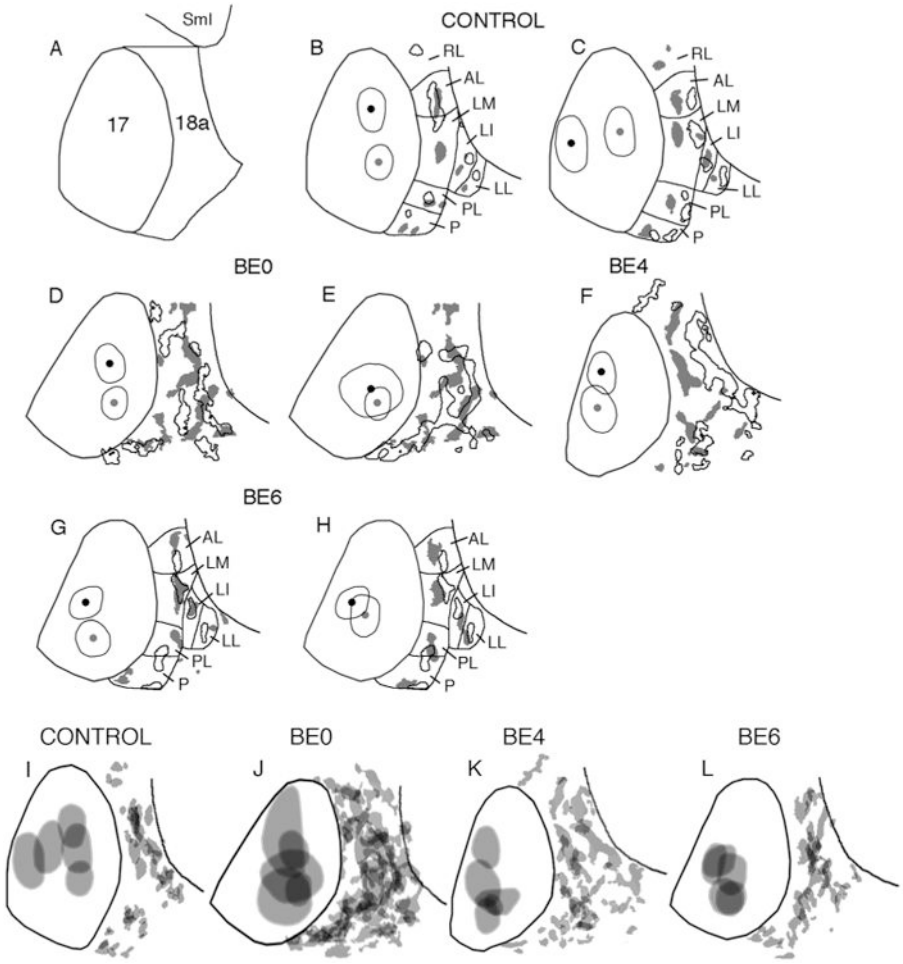

Figure 4.

A: Diagram illustrating the borders of area 18a in both control and enucleated rats, as defined by criteria used in this study (see Materials and Methods). Lateral is to the right, anterior is up. **B–H:** Comparison of 18a projection patterns from pairs of animals with BDA injections in different loci within striate cortex. Black outlines in area 18a indicate projections from injection sites marked by black dot and thin outline in area 17; gray patches in area 18a indicate projections from injection sites marked by gray dot and thin outline in area 17. Lateral border of area 18a is indicated by black line. Control (B,C); BE0 (D,E); BE4 (F); BE6 (G,H). **I–L:** Variability of the patterns of projections from striate cortex to lateral extrastriate cortex in control (I) and enucleated rats (J–L). The injection sites within striate cortex and the striate–extrastriate projection patterns in each group shown in Figure 3 were merged after their orientation had been adjusted so that the lateral border of striate cortex coincided as closely as possible within each group. The lateral border of area 18a is indicated by a black line. SmI, Somatosensory cortex; lateral extrastriate visual areas are named as reported previously: RL, rostrolateral; AL, anterolateral; LM, lateromedial; LI, laterointermediate; LL, laterolateral; PL, posterolateral; P, posterior (Olavarria and Montero, 1981, 1984, 1989; Espinoza and Thomas, 1983; Thomas and Espinoza, 1987; Montero, 1993; Coogan and Burkhalter, 1993; Wang and Burkhalter, 2007); other conventions as in Figure 3.

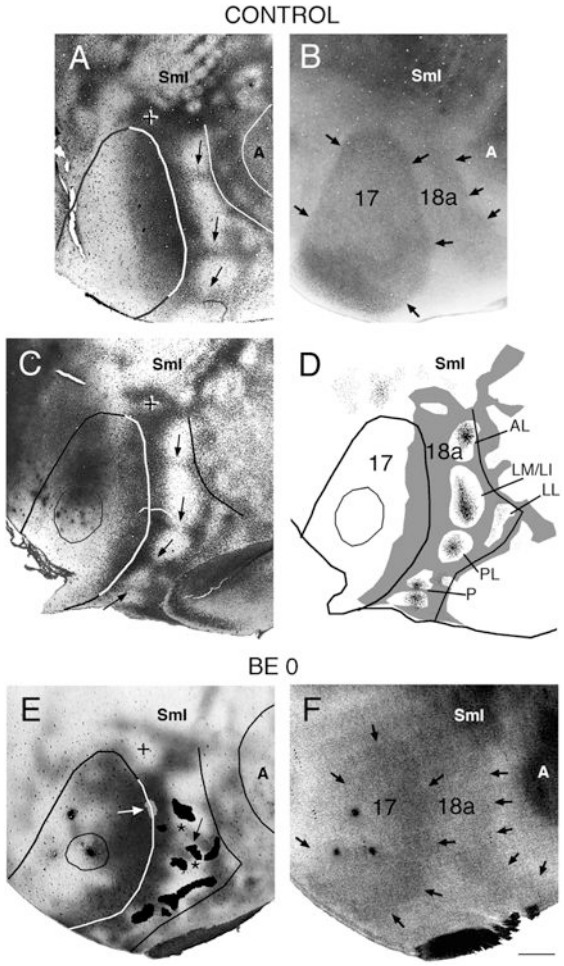

Figure 5.

Correlating the patterns of striate–extrastriate and visual callosal connections. Lateral is to the right, anterior is up. **A,B:** Callosal (A) and myelin (B) patterns in normal adult rat. In A, dark areas correspond to dense accumulations of retrogradely labeled somas and anterogradely labeled axons; the profiles of areas 17, 18a, and auditory cortex were drawn following myelin boundaries in the myelin pattern (B). Arrows in A indicate callosal bridges across area 18a, which separate several acallosal ring-like regions; the cross indicates the anterior callosal ring (Olavarria and Montero, 1984); black arrows in B indicate myelin boundaries. **C:** Callosal pattern in normal adult rat. Arrows point to callosal bridges separating several acallosal ring-like regions in area 18a. The cross indicates the anterior callosal ring. **D:** Thresholded version of callosal pattern in C is shown in gray. Fine black dots in extrastriate cortex indicate anterograde transport of tritiated proline from an injection of this tracer into striate cortex (thin outline). Lateral border of area 18a is delineated by black line. (Modified from Olavarria and Montero, 1984). **E:** Callosal pattern revealed following multiple injections of HRP in adult rat enucleated at birth. Dark areas correspond to dense accumulations of retrogradely labeled somas and anterogradely labeled axons. The cross indicates the anterior callosal ring. Asterisks mark two interrupted callosal bridges; striate–extrastriate projections are represented as black patches in area 18a, and arrow indicates striate projection field “wedged” between the two interrupted callosal bridges. White arrow points to small projection field (gray) contained in an area of reduced callosal labeling at the 17/18a border. The profiles of areas 17, 18a, and auditory cortex were drawn

from the callosal pattern in E and the myelin pattern in F. **F:** Myelin pattern from case shown in E. Arrows indicate borders of areas 17 and 18a. A, auditory cortex; other conventions as in Figure 4. Scale bar = 1.0 mm.

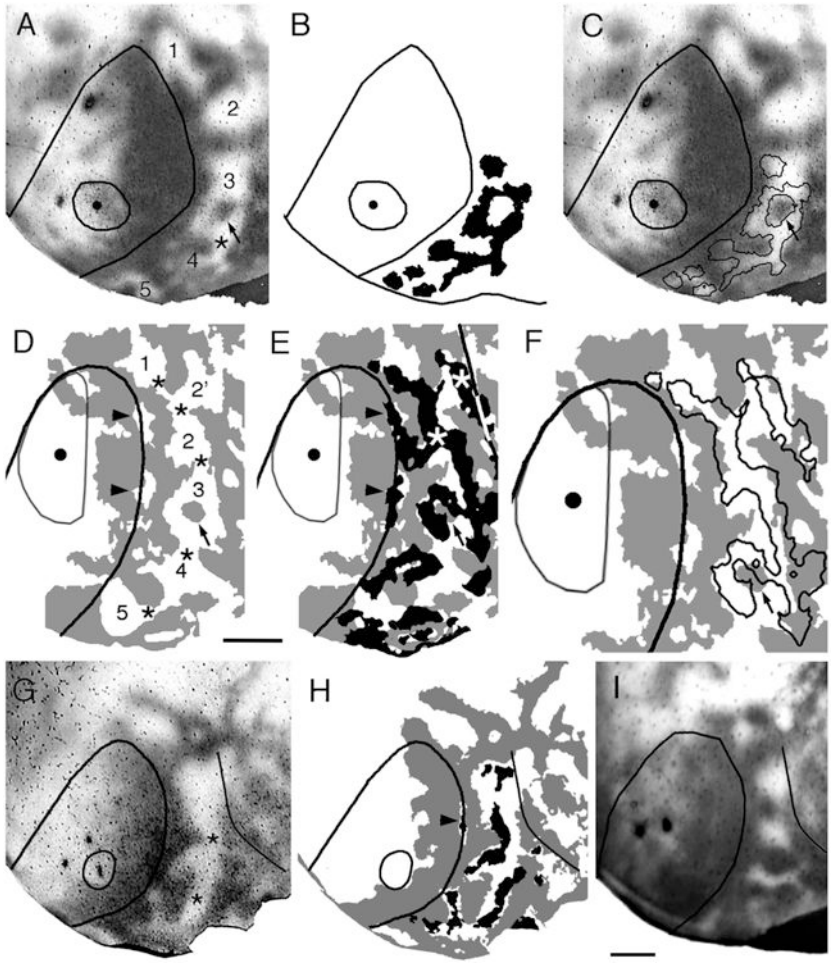

Figure 6.

Correlating the patterns of striate–extrastriate and visual callosal connections. The callosal patterns were revealed in adult rats following multiple injections of HRP in the contralateral hemisphere, and the striate–extrastriate projections were revealed following single injections of BDA into striate cortex. Injection site is represented by the dot and the fine outline. Lateral is to the right, anterior is up. **A–C:** Rat enucleated at birth. Dark areas in A,C correspond to dense accumulations of retrogradely labeled callosal somas and anterogradely labeled callosal axons. Numbers in A indicate acallosal regions. Asterisk in A indicates interrupted callosal bridge. Arrows in A,C indicate an island of densely labeled callosal connections. Striate–extrastriate projections are represented in black in B, and as outlines in C. **D–F:** Rat enucleated at birth. Callosal pattern is represented in gray. Striate–extrastriate projections are represented in black in E and as outlines in F. Numbers in D represent acallosal islands. Asterisks in D mark interrupted callosal bridges. Arrow in D–F marks an island of densely labeled callosal connections. Arrowheads in D mark acallosal regions at the 17/18a border, while arrowheads in E mark anomalous striate projections into these 17/18a acallosal regions. A portion of the lateral border of area 18a is indicated by a black/white line in E. **G:** Callosal pattern revealed following multiple injections of HRP in adult rat enucleated at birth. Dark areas correspond to dense accumulations of retrogradely labeled somas and anterogradely labeled axons. **H:** Thresholded version of callosal pattern in G is shown in gray. Black areas in extrastriate cortex indicate anterograde transport of BDA from an injection of this tracer into striate cortex (thin outline). Arrowhead points to a small

projection field within an area of reduced callosal connections at the 17/18a border. **I:** Callosal pattern in adult rat enucleated at P4. Lateral border of area 18a is indicated by black line in G–I. Scale bars = 1.0 mm.

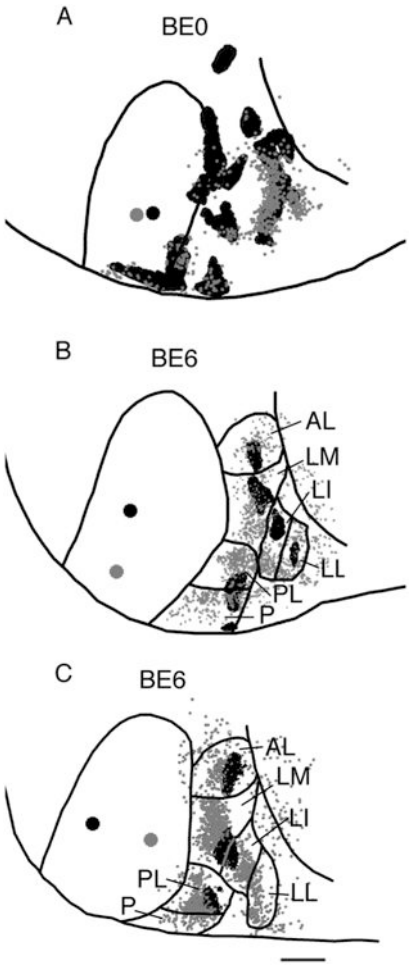

Figure 7.

Feedforward and feedback patterns of connections in area 18a of rats enucleated at P0 (BE0) **(A)** and P6 (BE6) **(B,C).** Lateral is to the right, anterior is up. Lateral border of area 18a is indicated by a black line. Large black dot in striate cortex represents a single injection of BDA, while the gray dot represents a single injection of rhodamine latex beads. Anterograde projections in area 18a are represented by the black areas, while the small gray dots represent cells labeled retrogradely by the transport of rhodamine latex beads. Visual areas are named as in Figure 4. Scale bar = 1.0 mm.

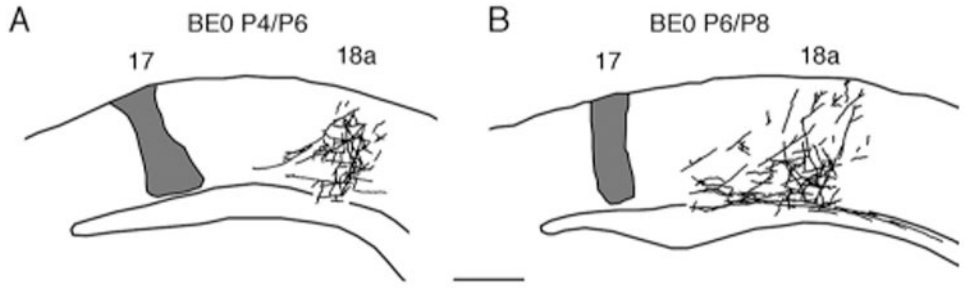

Figure 8.

Development of 17–18a projections in rats enucleated at birth. Lateral is to the right. Projections were studied following single injections of BDA into area 17 and the distribution of anterogradely labeled fibers was studied 48 hours later in coronal sections cut through occipital cortex. The injection site is represented in gray and labeled fibers are represented as black lines. **A:** Case injected at P4 and studied at P6. **B:** Case injected at P6 and studied at P8. Scale bar = 0.5 mm.

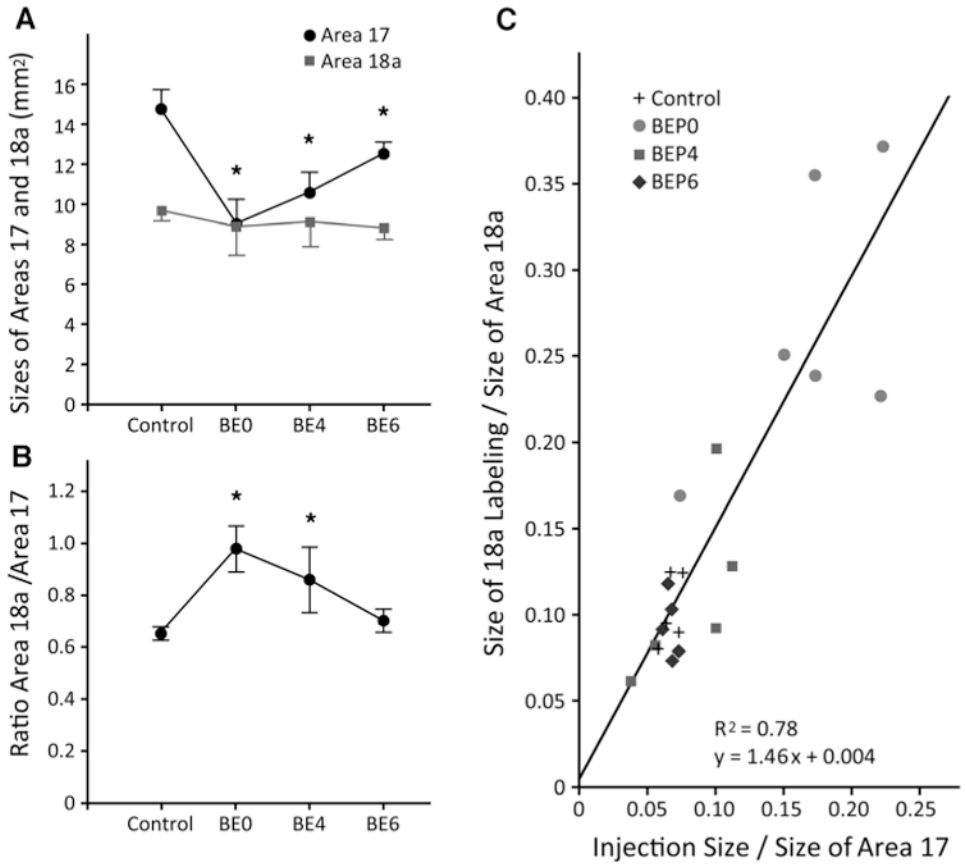

Figure 9.

A: Comparison of the sizes of areas 17 and 18a in control and in BE0, BE4, and B6 rats. Asterisks indicate that area 17 was significantly ($P < 0.05$) larger in control compared to each group of enucleated rats. In contrast, area 18a was not significantly different in control rats compared to any of the groups of enucleated rats. Error bars indicate SD. **B:** Comparison of the ratio of the size of area 18a to the size of area 17 in control and in BE0, BE4, and B6 rats. Asterisks indicate that this ratio was significantly ($P < 0.05$) smaller in control compared to BE0 and BE4 rats. Error bars indicate SD. **C:** Scatterplot correlating the overall proportion of area 18a occupied by the BDA-labeled projection from area 17 with the proportion of area 17 occupied by the injection of BDA into area 17.

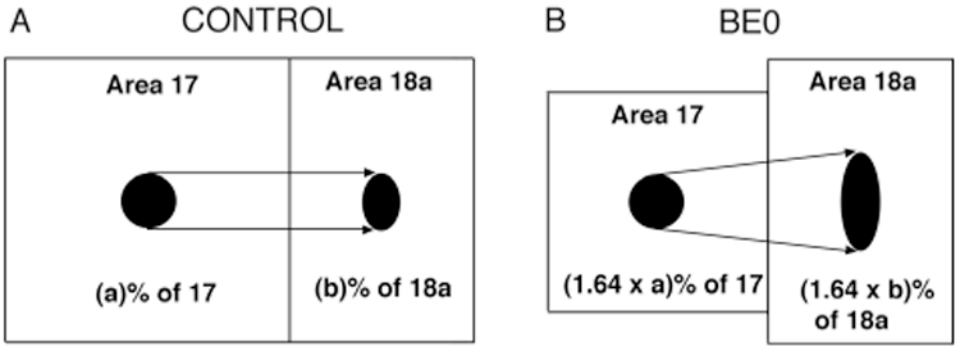

Figure 10.

Diagram summarizing the effects of BE0 on the sizes of areas 17 and 18a, and on the relation between the overall proportion of area 18a occupied by BDA labeling and the proportion of area 17 occupied by the BDA injection. The diagram illustrates that, on average, BE0 causes a 39% reduction in the size of area 17, while it does not have a significant effect on the size of area 18a. The BDA injection in area 17 of the control case **(A),** represented by the black circle, occupies (a)% of area 17, while in the BE0 case **(B),** the proportion of area 17 occupied by an injection of the same size increases by a factor of 1.64 due to the reduction in the size of area 17. For example, if the injection site occupied 10% of area 17 in the control rat, an injection of the same size would occupy 16.4% of area 17 in the B0 rat. Similarly, the proportion (b%) of area 18a occupied by the projection from area 17 in control rats (black oval in area 18a, panel A) increases by the same factor in area 18a of BE0 rats (black oval in area 18a, panel B). Thus, the diagram in B illustrates that, for an injection of the same size, the absolute size of the BDA labeling in area 18a is greater in BE0 than in control rats (cf. black ovals in areas 18a in A,B), indicating that enucleation leads to an increase in the divergence of the projections from 17 to 18a.